A Contour-Based Approach to the Multimode Network Representation of Waveguide Transitions

Werner L. Schroeder, *Member, IEEE,* and Marco Guglielmi

***Abstract*— A flexible and efficient numerical method is presented by which the multimode network representation (MMNR) of the abrupt transition between a standard waveguide and a waveguide of arbitrary cross section can be established without reference to the cross-sectional fields. The approach combines the boundary integral-equation method (BIEM) with contour integral expressions for the coupling coefficients, and a novel highly efficient scheme to express modal normalization constants in terms of coupling coefficients and eigenvalues. Application is demonstrated for a variety of multiridge circular waveguide (MRCW) configurations and transitions between MRCW and circular waveguide (CW). Comparison is made against most published results for this problem.**

***Index Terms*— Boundary integral equations, circular waveguides, *dual-mode* waveguide filters, mode-matching methods, waveguide discontinuities.**

I. Introduction

THE multimode network representation (MMNR) is well established as a rigorous approach to the analysis of cascaded waveguides of different cross sections [1]. By decomposing the problem, such as to leave the EMF analysis part (determination of cutoff frequencies and modal coupling coefficients) frequency independent and only a relatively simple multimode transmission-line network analysis frequency dependent, it is also very efficient, while identical to the mode-matching technique with respect to the field representation.

The application of the MMNR to standard waveguides with analytically known modal fields is straightforward. However, in the general case, it is often a numerical challenge. One aspect is the large number of modes which is required to obtain sufficient accuracy. Another aspect is the sensitivity of the computed overall frequency response of typical waveguide components to small variations of the cross-sectional geometry and, hence, to inexact representations of the latter. Finally, for design purposes, analysis is to be repeated with different geometrical parameters in an optimization loop. Since variation of geometrical parameters implies different discretizations, it is mandatory to assure a uniform convergence behavior, in particular, in the presence of TM-mode field singularities about reentrant corners.

Manuscript received June 17, 1997; revised January 14, 1998. This work was supported by the European Space Agency.

W. L. Schroeder is with the Department of Electrical Engineering, Duisburg University, D-47048 Duisburg, Germany (e-mail: werner@ate.uni-duisburg.de).

M. Guglielmi is with the RF System Division, European Space Research and Technology Centre, 2200 AG Noordwijk, The Netherlands.

Publisher Item Identifier S 0018-9480(98)02765-3.

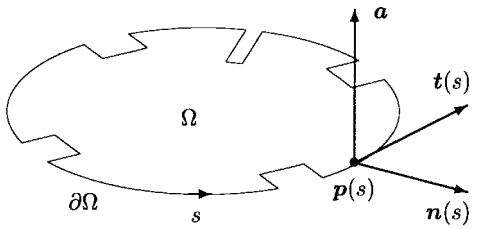

Fig. 1. Perspective view on the cross section Ω of a nonstandard waveguide with contour $\partial\Omega$ and moving tripod of unit vectors $(\mathbf{n}, \mathbf{t}, \mathbf{a})$ where $\mathbf{t} = \frac{d}{ds}\mathbf{p}$ and $\mathbf{n} = \mathbf{t} \times \mathbf{a}$.

An application for which these difficulties are all but trivial is the MMNR of the abrupt transition between a circular waveguide (CW) and a multiridge circular waveguide (MRCW) (see Fig. 1), which has recently found widespread interest in connection with efforts to design CW dual-mode filters without tuning screws. The replacement of tuning screws by an exactly premachined section of MRCW was proposed in [2]. Although alternative design concepts for dual-mode filters which avoid nonstandard waveguide cross sections have recently been presented [3], [4], the analysis of CW-MRCW transitions is taken as a test case for the present method.

Among the methods which have previously been used in this context are the finite-element method (FEM) [2]–[5], the radial method of lines [6], and the radial mode-matching method [7]–[9]. The latter are restricted to waveguide cross sections which conform to the coordinate lines of a cylindrical coordinate system, which allows for separation of variables. The FEM allows for approximate description of arbitrary cross sections. However, it may be counted as a disadvantage that the numerically most efficient contour integral expressions for the coupling coefficients [10] cannot be applied without loss of accuracy. The reason is that the FEM yields a weak solution for the domain, but has an ultimately unspecified local error along the (nonsmooth) contour. However, minimization of the error with respect to contour values is an inherent property of contour integral approaches. Such an approach was used in [11] to compute the first few TE modes of ridged waveguides with two symmetry planes. However, analysis of TM modes, which introduces the additional problem of field singularities, and evaluation of coupling coefficients were not considered.

Another approach [12] starts from an approximation of a Green's function for a similar standard waveguide cross

section to arrive at an algebraic eigenvalue problem. This feature makes the approach numerically effective, particularly if only a moderate number of modes is desired. However, for a large number of modes, accurate approximation of the Green's function becomes more difficult, and uniqueness of the solution may also present a problem [13].

This paper is based on the boundary integral-equation method (BIEM) which has previously been applied to TM-, TE-, and hybrid-mode analysis of a variety of guided wave structures, including media with finite conductivity [14]–[16]. Unique features of this method are its capability to represent an arbitrarily curved waveguide contour without resorting to staircase or polygonal approximations, and the simplicity by which field singularities can be accounted for with asymptotically exact expansions functions. Both features are of specific importance within an optimization loop to assure uniform accuracy over all geometrical parameters which may be encountered.

II. Modal Analysis

To define the notation which is to be used in subsequent derivations, the representation of TM and TE modes in hollow waveguides is briefly summarized. Single primed symbols refer to TM modes; double primed symbols to TE modes. Expressions which hold in identical form for TM- and TE-mode quantities are written only once with the primes omitted.

A. Representations of Modal Fields

TM and TE modes will be described in terms of axially oriented *Hertzian potentials* $\mathbf{a}\psi'_n$ and $\mathbf{a}\psi''_n$. $\mathbf{a}$ denotes the axial unit vector (see Fig. 1). The functions $\psi_n : \Omega \to \mathbb{R}$ solve

$$\Delta\psi_n + h_n^2\psi = 0 \tag{1}$$

with eigenvalues h'_n for Dirichlet boundary conditions and eigenvalues h''_n for Neumann boundary condition. The orthogonality relations between the solutions of (1) will be used in the form

$$\langle \nabla\psi'_n, \nabla\psi'_m\rangle_\Omega = \left(P'_n\right)^2\delta_{nm} \tag{2}$$

$$\langle \nabla\psi''_n, \nabla\psi''_m\rangle_\Omega = \left(P''_n\right)^2\delta_{nm} \tag{3}$$

$$\langle \nabla\psi''_n, \mathbf{a}\times\nabla\psi'_m\rangle = 0, \qquad \text{for } m,n \in \mathbb{N}. \tag{4}$$

The normalized transverse modal fields will be denoted by

$$\mathbf{e}'_n := \frac{1}{P'_n}\nabla\psi'_n \quad \mathbf{h}'_n := \mathbf{a}\times\mathbf{e}'_n \tag{5}$$

and

$$\mathbf{h}''_n := \frac{1}{P''_n}\nabla\psi''_n \quad \mathbf{e}''_n := \mathbf{h}''_n\times\mathbf{a}. \tag{6}$$

The modal decomposition of the full 3-D electromagnetic field is the starting point of the MMNR. However, it should be noted that the description of TM and TE modes in terms of Hertzian potentials or transverse fields is still highly redundant. All information about a mode which can be written as a linear functional of the transverse fields can equivalently be written as a linear functional of its boundary values only. It is, therefore, possible to go one step beyond the reduction from three-dimensional (3-D) to two-dimensional (2-D) fields and formulate the problem exclusively in terms of simple one-dimensional (1-D) functions. To this end, we introduce as a generalization of the boundary values of a Hertzian potential, its *traces* with respect to some closed contour $\Gamma \subset \bar{\Omega}$. Let

$$\mathbf{p} : I \to \Gamma, \qquad s \mapsto \mathbf{p}(s) \tag{7}$$

denote the parameterization of Γ in terms of arc length $s \in I \subset \mathbb{R}$. Further, let $\dot{I}$ denote the interval I with the exception of the (finite) number of singular points where the tangent along Γ is discontinuous. The normal vector along Γ may then be defined as

$$\mathbf{n} : \dot{I} \to \mathbb{R}^2, \qquad s \mapsto -\mathbf{a}\times\frac{\partial}{\partial s}\mathbf{p}(s). \tag{8}$$

With these definitions, we introduce the *traces* of ψ_n with respect to Γ as

$$u_n : I \to \mathbb{R}, \qquad s \mapsto \psi_n(\mathbf{p}(s)) \tag{9}$$

and

$$v_n : \dot{I} \to \mathbb{R}, \qquad s \mapsto \mathbf{n}\nabla_{\mathbf{p}}\psi_n(\mathbf{p}(s)). \tag{10}$$

The traces coincide with the boundary values of the Hertzian potential and those of its normal derivative, respectively, if Γ is identified with waveguide contour $\partial\Omega$. It is then obvious that each mode is completely described by eigenvalue and trace. An illustration of this representation is given in Fig. 2. Attractive features of the purely 1-D representation are the exact parametric representation of an arbitrarily curved waveguide contour, the small number of expansion functions, and the simplicity by which edge terms with the asymptotically exact singular behavior can be included.

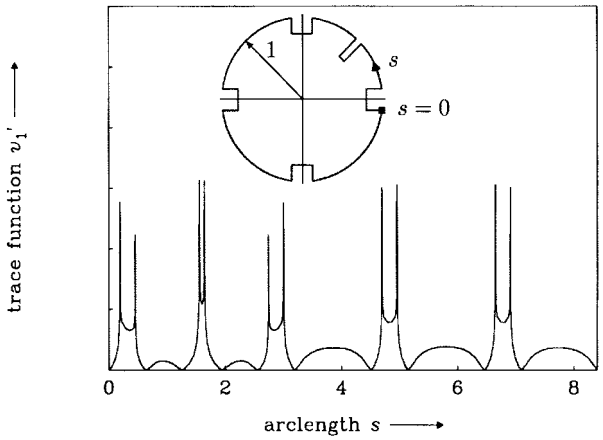

Fig. 2. Trace function v'_1 of the first TM mode for the MRCW shown in the inset (arbitrary units).

B. Trace-Function Eigenvalue Problem

To exploit these advantages, one has to reformulate the eigenvalue problem (1) for the Hertz potentials as an eigenvalue problem for the trace functions. By application of Green's second identity to ψ_n and a suitably chosen fundamental solution of (1), we arrive at a homogeneous contour integral

TABLE I
GEOMETRICAL PARAMETERS OF MRCW CONFIGURATIONS A–J. FOR MEANING OF SYMBOLS, SEE TEXT AND FIG. 3

	config. code	ridge shape	d_h	b_h	d_v	b_v	d_c	b_c	Ref.
A	01010101	rectangular	parameter	0.2610524	d_h	0.2610524	–	–	[2]
B	01010101	rectangular	parameter	0.12	d_h	0.12	–	–	[11]
C	01010111	rectangular	0.8	0.2610524	0.8	0.2610524	0.0872388	parameter	[2]
D	01010111	circular	parameter	–	0.7	–	0.9	–	–
E	10001000	rectangular	–	–	0.500	0.03125	–	–	[9]
F	10001000	conical	–	–	parameter	0.0348995	–	–	[9]
G	00000111	rectangular	0.8633334	0.1666667	0.85	0.1666667	0.7733334	0.1666667	[12]

equation for the trace functions. Since we are interested in arbitrary waveguide cross sections, we choose the free-space Green's function

$$g_h : I \times I \backslash \operatorname{diag} I \times I \to \mathbb{C}, \qquad (t,s) \mapsto K_0(jh\|\mathbf{r}(t,s)\|) \tag{11}$$

where K_0 denotes the modified Bessel function of the second kind and zeroth order and $\mathbf{r}(t,s) := \mathbf{p}(t) - \mathbf{p}(s)$. Splitting $g(t,s)$ into its singular part, $g_0(t,s) := -\ln(\|\mathbf{r}(t,s)\|)$ and the remaining regular part $\tilde{g}_h(t,s)$, the trace-function eigenvalue problems take the form [14]

$$\mathbf{G}_{h'}[v'](t) := \int_{\dot{I}\backslash\{t\}} g_0(t,s)v'(s)\,ds + \int_{\dot{I}\backslash\{t\}} \tilde{g}_{h'}(t,s)v'(s)\,ds = 0 \tag{12}$$

for the TM modes and

$$\mathbf{K}_{h''}[u''](t) := \int_{\dot{I}\backslash\{t\}} (u''(s) - u''(t))\,k_0(t,s)\,ds + \int_{\dot{I}} u''(s)\tilde{k}_{h''}(t,s)\,ds = 0 \tag{13}$$

for TE modes. In both equations, it is understood that I maps on $\Gamma = \partial\Omega$. The kernels

$$k_0(t,s) := \frac{\mathbf{r}(t,s)\mathbf{n}(s)}{\|\mathbf{r}(t,s)\|} \tag{14}$$

and

$$\tilde{k}_h(t,s) := (jhK_1(jh\|\mathbf{r}(t,s)\|) - 1)k_0(t,s) \tag{15}$$

are the (source point) normal derivatives of g_0 and $\tilde{g}_h$. The operators $\mathbf{G}_{h'}$ and $\mathbf{K}_{h''}$ are to be approximated by finite dimensional-matrix operators upon selection of a suitable expansion of the trace functions. With view on numerical integration, we have, therefore, decomposed the contour integrals appearing in (12) and (13) into contributions due to the singular and regular part of the fundamental solution. This decomposition and the particular form of the first term in (13) are mandatory to assure uniform convergence of the integrals on the right-hand side of (13) if both s and t approach a singular point. A more detailed discussion of this problem can be found in [14]. In (12), the decomposition is still advantageous from a numerical point of view because only the first integral is (weakly) singular, but on the other hand,

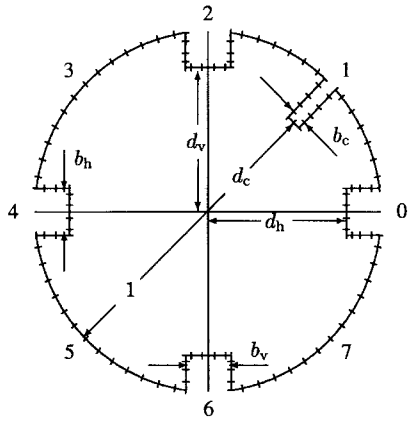

Fig. 3. Definition of geometrical parameters for MRCW configurations A–G of Table I. The figure applies as is to configuration C and also shows the partition of the contour.

independent from the transverse wavenumber h'_n and, hence, to be evaluated only once for a given waveguide contour.

Discretization of the operators $\mathbf{G}_{h'}$ and $\mathbf{K}_{h''}$ is accomplished by expanding the traces into second-order B-splines, for v' augmented by edge terms with a singularity of order $\tau = \frac{\pi}{\gamma} - 1 > \frac{1}{2}$ about a reentrant corner of angle γ. Fig. 3 shows a typical nonequidistant partition of the waveguide contour. A regular B-spline extends over three elements of the partition. Numerical integration is performed on an element by element basis using an adaptive iteration scheme. A nonlinear substitution first removes the singularities of the fundamental solution and the expansion functions. A modified Romberg scheme is then applied to evaluate the integral up to the specified relative error. The advantage of this procedure over fixed-order integration rules is the decoupling of integration error and spatial resolution. In connection with the parametric representation of the waveguide contour, it lends to an automatic refinement of the geometrical approximation until the specified relative integration error (typically 10^{-7}) is met.

The residuals of the operator equations are tested using the *method of least squares with intermediate projection*, an approach which assures the absence of spurious solutions [17]. The method uses two weighting functions per expansion function. The resultant nonsquare matrix operator is subject to singular-value decomposition to locate the eigenvalues as minima of the residual. Like all other numerical approaches which end up in a search procedure for eigenvalues, the present approach is (at this point) faced with the problem to reliably detect arbitrarily close eigenvalues. This problem has been solved by a novel multiple eigenvalue search algorithm

(MESA). It is based on simultaneous consideration of several singular vectors as possible candidate solutions, making use of the fact that the solution vectors for degenerate eigenvalues are orthogonal. Degenerate solutions can, therefore, be identified as near zeros of the residuals (i.e., the singular values) of two or more singular vectors. It can be shown that the singular vectors corresponding to two closely neighbored eigenvalues—though not strictly orthogonal—are still almost orthogonal. Because of the analytic dependence of the Green's function on transverse wavenumber, it is in fact possible to write the inner product between the singular vectors which correspond to two closely neighbored eigenvalues as a power series in eigenvalue separation. This property makes it possible to establish a correlation between subsequent samples of singular values by comparing inner products between the corresponding solution vectors. The sets of singular values obtained at different sampling points can thus be interpreted as sampling values of a set of *continuous* residual functions, each bound to one of a set of continuously evolving candidate solutions which are locally mutually orthogonal. This approach puts the detection of closely spaced eigenvalues on the same footage as that of degenerate eigenvalues. The method was found to allow for reliable detection of hundreds of eigenvalues without any *a priori* information on their separation. In addition, it results in a dramatic increase of numerical efficiency because the sampling step width is no longer bounded by eigenvalue separation, but only by the width of the minima of the residual functions. The number of initial sampling steps is thereby typically reduced to the number of eigenvalues to be detected. The approach may equally well be applied within other numerical methods for electromagnetic-field eigenvalue problems which amount to the solution of a nonlinear, as opposed to algebraic eigenvalue problem. A detailed derivation of the MESA in a more general context and a description of its implementation will be presented in a separate paper.

III. Coupling Coefficients

This section derives expressions for the coupling coefficients between TM and TE modes of two waveguides of different cross sections in terms of traces and eigenvalues. Following a brief summary of the relevant definitions, we shall consider the case where one of the waveguides is a standard waveguide with separable cross section Ω^O, chosen such that the arbitrary cross section Ω^I is contained in the closure of Ω^O. The general case of two arbitrary cross sections Ω^I and Ω^{II} just lends to a simple and obvious algebraic expression in terms of the coupling matrices derived for the $\Omega^O - \Omega^I$ and $\Omega^O - \Omega^{II}$ transitions. Below, superscripts ^{O} and ^{I} will be placed on quantities which relate to cross section Ω^O and Ω^I, respectively.

A. Definition of Coupling Coefficients

Observing that the sets of transverse modal fields

$$\mathcal{E}^O := \{\mathbf{e}_m^{O\prime} : m \in \mathbb{N}\} \cup \{\mathbf{e}_n^{O\prime\prime} : n \in \mathbb{N}\} \tag{16}$$

$$\mathcal{H}^I := \{\mathbf{h}_m^{I\prime} : m \in \mathbb{N}\} \cup \{\mathbf{h}_n^{I\prime\prime} : n \in \mathbb{N}\} \tag{17}$$

are orthonormal bases of $L_2(\Omega^O, \mathbb{R}^2)$ and $L_2(\Omega^I, \mathbb{R}^2)$, respectively, the continuity conditions for the total transverse fields

$$\begin{pmatrix} \mathbf{E}_{\mathrm{trv}} \\ \mathbf{H}_{\mathrm{trv}} \end{pmatrix} = \sum_{m=1}^{\infty} \begin{pmatrix} V_m' \mathbf{e}_m' \\ I_m' \mathbf{h}_m' \end{pmatrix} + \sum_{n=1}^{\infty} \begin{pmatrix} V_n'' \mathbf{e}_n'' \\ I_n'' \mathbf{h}_n'' \end{pmatrix} \tag{18}$$

in the common interface plane of both waveguides lends to the infinite system of equations

$$\left\langle \mathbf{e}, \mathbf{E}_{\mathrm{trv}}^O - \mathbf{E}_{\mathrm{trv}}^I \right\rangle_{\Omega^O} = 0 \quad \forall \mathbf{e} \in \mathcal{E}^O \tag{19}$$

$$\left\langle \mathbf{h}, \mathbf{H}_{\mathrm{trv}}^O - \mathbf{H}_{\mathrm{trv}}^I \right\rangle_{\Omega^I} = 0 \quad \forall \mathbf{h} \in \mathcal{H}^I. \tag{20}$$

$\langle \cdot, \cdot \rangle_\Omega$ denotes the symmetric inner product with respect to Ω. The domain of definition of $\mathbf{E}_{\mathrm{trv}}^I$ has tacitly been extended to Ω^O with $\mathbf{E}_{\mathrm{trv}}^I \equiv 0$ on $\Omega^O \backslash \Omega^I$ to simplify the notation. Substitution of (18) and exploitation of the orthogonality relations (2)–(4) yields (after restriction to finite numbers of modes) the well-known matrix equations

$$\begin{pmatrix} \mathbf{V}^{O\prime} \\ \mathbf{V}^{O\prime\prime} \end{pmatrix} = \begin{pmatrix} \mathbf{C}' & \mathbf{C}''' \\ \mathbf{0} & \mathbf{C}'' \end{pmatrix} \begin{pmatrix} \mathbf{V}^{I\prime} \\ \mathbf{V}^{I\prime\prime} \end{pmatrix} \tag{21}$$

and

$$\begin{pmatrix} \mathbf{C}'^{\top} & \mathbf{0} \\ \mathbf{C}'''^{\top} & \mathbf{C}''^{\top} \end{pmatrix} \begin{pmatrix} \mathbf{I}^{O\prime} \\ \mathbf{I}^{O\prime\prime} \end{pmatrix} = \begin{pmatrix} \mathbf{I}^{I\prime} \\ \mathbf{I}^{I\prime\prime} \end{pmatrix} \tag{22}$$

where the $\mathbf{V}$ and $\mathbf{I}$ denote the vectors of modal voltages and currents. $\mathbf{C}'$, $\mathbf{C}'''$, $\mathbf{C}''$ are the *coupling matrices* with elements

$$c'_{mn} = \left\langle \mathbf{e}_m^{O\prime}, \mathbf{e}_n^{I\prime} \right\rangle_{\Omega^I} = \frac{1}{P_m^{O\prime} P_n^{I\prime}} \iint_{\Omega^I} \nabla \psi_m^{O\prime} \cdot \nabla \psi_n^{I\prime} \, d\Omega \tag{23}$$

corresponding to the mth TM mode in Ω^O and the nth TM mode in Ω^I as follows:

$$c'''_{mn} = \left\langle \mathbf{e}_m^{O\prime}, \mathbf{e}_n^{I\prime\prime} \right\rangle_{\Omega^I} = \frac{1}{P_m^{O\prime} P_n^{I\prime\prime}} \iint_{\Omega^I} \left(\mathbf{a} \times \nabla \psi_m^{O\prime} \right) \cdot \nabla \psi_n^{I\prime\prime} \, d\Omega \tag{24}$$

corresponding to the mth TM mode in Ω^O and the nth TE mode in Ω^I and

$$c''_{mn} = \left\langle \mathbf{e}_m^{O\prime\prime}, \mathbf{e}_n^{I\prime\prime} \right\rangle_{\Omega^I} = \frac{1}{P_m^{O\prime\prime} P_n^{I\prime\prime}} \iint_{\Omega^I} \nabla \psi_m^{O\prime\prime} \cdot \nabla \psi_n^{I\prime\prime} \, d\Omega \tag{25}$$

corresponding to the mth TE mode in Ω^O and the nth TE mode in Ω^I.

B. Coupling Coefficient in Terms of Traces

Expressions for the coupling coefficients in terms of contour integrals have previously been given [10]. A more concise argument is given below for the readers convenience. Noting that the expressions

$$\nabla(\varphi_1 \nabla \varphi_2 + \varphi_2 \nabla \varphi_1) = 2 \nabla \varphi_1 \cdot \nabla \varphi_2 - \left(h_1^2 + h_2^2\right) \varphi_1 \varphi_2 \tag{26}$$

and

$$\nabla(\varphi_1 \nabla \varphi_2 - \varphi_2 \nabla \varphi_1) = \left(h_1^2 - h_2^2\right) \varphi_1 \varphi_2 \tag{27}$$

are identities for any two functions φ_1, φ_2 which solve (1) in some region Ω with eigenvalues h_1 and h_2, respectively, we obtain by combination of (26) and (27)

$$\nabla\varphi_1 \cdot \nabla\varphi_2 = \nabla\left(\frac{h_1^2}{h_1^2 - h_2^2}\varphi_1\nabla\varphi_2 + \frac{h_2^2}{h_2^2 - h_1^2}\varphi_2\nabla\varphi_1\right). \quad (28)$$

Subsequent application of the divergence theorem lends to

$$\langle\nabla\varphi_1, \nabla\varphi_2\rangle_\Omega = \frac{h_1^2}{h_1^2 - h_2^2}[u_1, v_2]_I + \frac{h_2^2}{h_2^2 - h_1^2}[v_1, u_2]_I \quad (29)$$

where u_i and v_i, $i \in \{1, 2\}$ are the traces of φ_i with respect to $\Gamma = \partial\Omega$, as defined by (9) and (10). $[\cdot, \cdot]_I$ denotes the symmetric inner product with respect to the interval I, the domain of definition of the parameterization of Γ.

A second identity is obtained by applying the divergence theorem to

$$\nabla\varphi_1 \cdot (\nabla\varphi_2 \times \mathbf{a}) = \nabla(\varphi_1(\nabla\varphi_2 \times \mathbf{a})). \quad (30)$$

With the same definition of symbols as above, the result is

$$\langle\nabla\varphi_1, \nabla\varphi_2 \times \mathbf{a}\rangle_\Omega = \left[u_1, \frac{\partial u_2}{\partial s}\right]_I. \quad (31)$$

The desired expressions for the coupling coefficients in terms of the traces are now immediately obtained by applying (29) to the right-hand sides of (23) and (25), and likewise, (30) to the right-hand side of (24) upon identification of Ω with Ω^I. Since $u_n^{I\prime}$ and $v_n^{I\prime\prime}$ are both identically zero, the result simplifies to

$$c'_{mn} = \frac{1}{P_m^{O\prime}P_n^{I\prime}} \frac{\left(h_m^{O\prime}\right)^2}{\left(h_m^{O\prime}\right)^2 - \left(h_n^{I\prime}\right)^2}\left[u_m^{O\prime}, v_n^{I\prime}\right]_{I^I} \quad (32)$$

$$c'''_{mn} = -\frac{1}{P_m^{O\prime}P_n^{I\prime\prime}}\left[\frac{d}{ds}u_m^{O\prime}, u_n^{I\prime\prime}\right]_{I^I} \quad (33)$$

and

$$c''_{mn} = \frac{1}{P_m^{O\prime\prime}P_n^{I\prime\prime}} \frac{\left(h_n^{I\prime\prime}\right)^2}{\left(h_n^{I\prime\prime}\right)^2 - \left(h_m^{O\prime\prime}\right)^2}\left[v_m^{O\prime\prime}, u_n^{I\prime\prime}\right]_{I^I}. \quad (34)$$

The inner products in the above expressions can be evaluated with little numerical effort. Subsections of $\partial\Omega^I$ which are contained in $\partial\Omega^O$ do not make a contribution. Considering, for instance, a CW and a ridged waveguide, as shown in Fig. 1, the domain of integration reduces to the small subintervals of I^I, which map on the ridge boundaries. Moreover, since $u_m^{O\prime}$ and $v_m^{O\prime\prime}$ are assumed to be known analytically, while $v_n^{I\prime}$ and $u_n^{I\prime\prime}$ [obtained by solving (12) and (13)] are represented by coefficient vectors with respect to fixed expansion functions on I, numerical integrations are to be performed just once for each mode in Ω^O and each expansion function.

C. Mode Normalization

Expressions (32)–(34) still contain the so far unknown normalization constants $P_n^{I\prime}$ and $P_n^{I\prime\prime}$ for the nonstandard waveguide. Because the norm of a mode is a quadratic functional of the field, it is not possible to obtain the normalization constants in terms of single contour integrals over the traces, a fact which hitherto seemed to make the BIEM unattractive for the present application. Below, we present a novel approach to express the normalization constants in terms of eigenvalues and coupling coefficients for the nonnormalized modes at negligible extra numerical expense.

To derive the required expressions, recall that $\mathcal{E}^O$ is an orthonormal basis of $L_2(\Omega^O, \mathbb{R}^2)$ and that $\Omega^I \subset \bar{\Omega}^O$. By definition of the coupling coefficients, we may, therefore, expand the transverse fields of the nonstandard waveguide in the form

$$\mathbf{e}_n^{I\prime} = \sum_{j=1}^{\infty} c'_{jn}\mathbf{e}_j^{O\prime} \quad (35)$$

and

$$\mathbf{e}_n^{I\prime\prime} = \sum_{j=1}^{\infty} c'''_{jn}\mathbf{e}_j^{O\prime} + \sum_{i=1}^{\infty} c''_{in}\mathbf{e}_i^{O\prime\prime}. \quad (36)$$

The above expansions define continuations of the fields $\mathbf{e}_n^{I\prime}$ and $\mathbf{e}_n^{I\prime\prime}$ onto Ω^O with zero values on $\Omega^O \backslash \Omega^I$. It is possible, therefore, to express the norm of the transverse modal fields in the nonstandard waveguide in terms of the right-hand sides of (35) and (36).

The expansion (36) of the TE modes is considered first. The coupling coefficients appearing in (36) are the generalized Fourier coefficients of the continuation of $\mathbf{e}_n^{I\prime\prime}$ onto Ω^O with respect to the orthonormal system $\mathcal{E}^O$. Since the continuation of $\mathbf{e}_n^{I\prime\prime}$ onto Ω^O is bounded, and furthermore continuous almost everywhere on Ω^O, it follows that the coefficients are square-summable, and by exploitation of the orthonormality of the modes in either waveguide we obtain Parseval's formula in the form

$$\left\langle\mathbf{e}_n^{I\prime\prime}, \mathbf{e}_n^{I\prime\prime}\right\rangle_{\Omega^I} = \sum_{j=1}^{\infty}(c'''_{jn})^2 + \sum_{i=1}^{\infty}\left(c''_{in}\right)^2 = 1. \quad (37)$$

This equation applies to the properly normalized coupling coefficients as defined by (32)–(34). If only the coupling coefficients $\tilde{c}'''_{jn} := P_n^{I\prime\prime}c'''_{jn}$ and $\tilde{c}''_{in} := P_n^{I\prime\prime}c''_{in}$, evaluated for nonnormalized modes in Ω^I are available, the above relation obviously provides a quadrature formula. Restricting to finite numbers of $M^{O\prime}$ TM and $M^{O\prime\prime}$ TE modes in Ω^O, it reads

$$\left(P_n^{I\prime\prime}\right)^2 \approx \sum_{j=1}^{M^{O\prime}}\left(\tilde{c}'''_{jn}\right)^2 + \sum_{i=1}^{M^{O\prime\prime}}\left(\tilde{c}''_{in}\right)^2. \quad (38)$$

The evaluation of the norms of TM-mode fields in Ω^I requires some additional consideration. Because the continuation of the TM-mode fields $\mathbf{e}_n^{I\prime}$ of the nonstandard waveguide onto Ω^O is, in general, not bounded, it is not possible to interchange the order of integration and summation on the right-hand side of the expression

$$\left\langle\mathbf{e}_n^{I\prime}, \mathbf{e}_n^{I\prime}\right\rangle_{\Omega^I} = \left\langle\sum_{i=1}^{\infty}c'_{in}\mathbf{e}_i^{O\prime}, \sum_{j=1}^{\infty}c'_{jn}\mathbf{e}_j^{O\prime}\right\rangle_{\Omega^O}. \quad (39)$$

The sequence of partial sums $\sum_{j=1}^{N}(c'_{jn})^2, N \in \mathbb{N}$ has, in fact, no limit. The problem can be solved by considering the norm of the Hertzian potential $\psi_n^{I\prime}$ instead. Generally, the norm of a

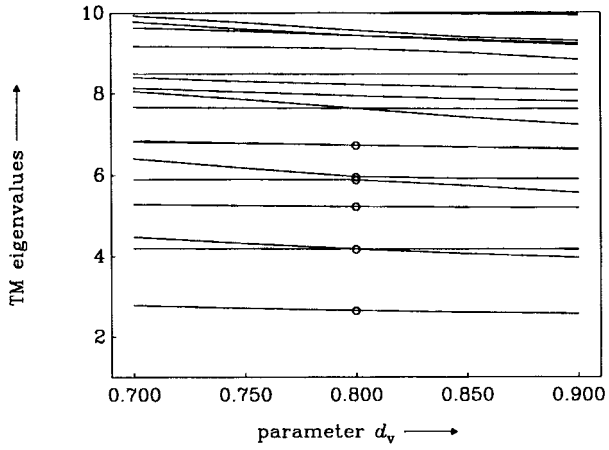

(a)

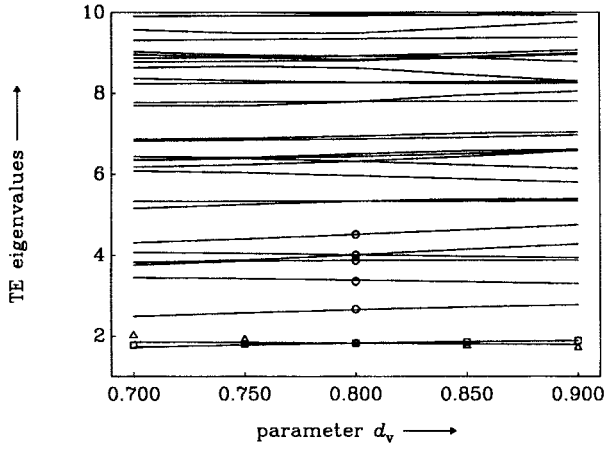

(b)

Fig. 4. Variation of (a) the first 19 TM-mode and (b) the first 30 TE-mode eigenvalues of configuration A with the length of the vertical tuning ridges. Symbols refer to results given in [2].

transverse modal field $\mathbf{e}_n$ of either type in a hollow waveguide and the norm of the Hertzian potential ψ_n from which it has been derived are related via

$$P_n^2\langle \mathbf{e}_n, \mathbf{e}_n\rangle = h_n^2\langle \psi_n, \psi_n\rangle \tag{40}$$

as a simple application of Green's first identity if the normalization defined by (2)–(6) is adopted.

Considering (5), (35), and the boundary conditions for the TM-mode Hertzian potentials $\psi_n^{I\prime}$ in Ω^I, it is easily verified that the latter have the series expansion

$$\frac{1}{P_n^{I\prime}}\psi_n^{I\prime} = \sum_{j=1}^{\infty} c'_{jn}\frac{1}{P_j^{O\prime}}\psi_j^{O\prime} \tag{41}$$

which, as opposed to (35), is uniformly convergent on $\bar{\Omega}^O$ because the continuation of $\psi_n^{I\prime}$ onto Ω^O with zero values on $\Omega^O\backslash\Omega^I$ is continuous everywhere.

Since $\{\psi_j^{O\prime} : j \in \mathbb{N}\}$ is an orthogonal set in $L_2(\Omega^O, \mathbb{R})$ it follows from (41) that

$$\left(\frac{1}{P_n^{I\prime}}\right)^2\langle \psi_n^{I\prime}, \psi_n^{I\prime}\rangle_{\Omega^I} = \sum_{j=1}^{\infty}\left(\frac{c'_{jn}}{P_j^{O\prime}}\right)^2\langle \psi_j^{O\prime}, \psi_j^{O\prime}\rangle_{\Omega^O}. \tag{42}$$

TABLE II
COMPARISON OF EIGENVALUES FOR CONFIGURATION A AGAINST RESULTS PRESENTED IN [2] FOR $d_v = 0.8$

	BIEM	[2]		BIEM	[2]
TM_1	2.65177	2.64350	TE_1	1.82936	1.82790
TM_2	4.17470	4.16310	TE_2	1.82936	1.82790
TM_3	4.17470	4.16310	TE_3	2.65501	2.66790
TM_4	5.22026	5.21290	TE_4	3.38548	3.35770
TM_5	5.87925	5.87220	TE_5	3.86856	3.87200
TM_6	5.96038	5.94440	TE_6	4.01011	4.00320
TM_7	6.72523	6.71160	TE_7	4.01011	4.00320
TM_8	6.72523	6.71160	TE_8	4.50831	4.51290

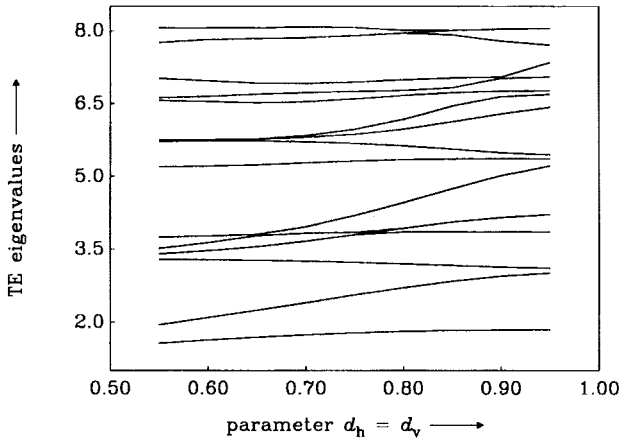

Fig. 5. Variation of the first 20 TE-mode eigenvalues of configuration B with the penetration of one pair of tuning ridges.

The combination of (40) and (42) lends to

$$\left(h_n^{I\prime}\right)^2\sum_{j=1}^{\infty}\left(\frac{c'_{jn}}{h_j^{O\prime}}\right)^2 = 1 \tag{43}$$

which is the desired normalization condition for the coupling coefficients. As before, a quadrature formula is obtained if the coupling coefficients $\tilde{c}'_{jn} := P_n^{I\prime}c'_{jn}$, computed for normalized modes in Ω^O, but nonnormalized modes in Ω^I, are substituted. Restricting to a finite number of $M^{O\prime}$ modes in Ω^O, the result is

$$\left(P_n^{I\prime}\right)^2 \approx \left(h_n^{I\prime}\right)^2\sum_{j=1}^{M^{O\prime}}\left(\frac{\tilde{c}'_{jn}}{h_j^{O\prime}}\right)^2. \tag{44}$$

It may be noted that the quadrature formulas (38) and (44) yield the desired normalization constants at almost no extra numerical expense. The error of the finite sum approximations in these formulas is just the error incurred by expanding a mode in Ω^I into a finite subset of the modes in Ω^O. The former is easily estimated by comparing the sequences of partial sums against the limiting value of a simple exponential fitting function. A relative error termination criterion for the summations in (38) and (44) is, therefore, also suitable to determine the number of modes which should be retained in Ω^O.

IV. NUMERICAL RESULTS

Application of the method is illustrated below for analysis of several MRCW configurations and CW-MRCW transitions.

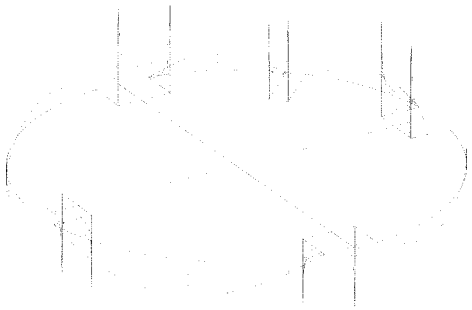

(a)

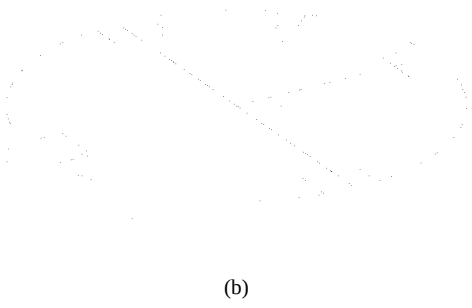

(b)

(c)

Fig. 6. (a) Trace function v'_{10} and (b) u''_{32} for the 10th TM and the 32nd TE mode of MRCW configuration C. (c) Trace function v'_1 (axial surface current density) for the first TM mode of configuration D with $d_h = 0.80$.

Their parameters are listed in Table I. The ridges are centered about the $n \times 45°$ positions along the unit circle. The *configuration code* in Table I specifies the occupied positions by a "1" as the nth binary digit. d_h (d_v, d_c) are the normalized distances between the origin and the tips of the horizontal (vertical, coupling) ridges, b_h (b_v, b_c) are the normalized widths of the ridges measured at their tips, as shown for configuration C in Fig. 3. In view of the limited amount of reference results which are currently available, and moreover because accuracy checks against analytically tractable examples are (due to the absence of reentrant corners and field singularities) inherently too optimistic, we include numerical tables for comparison against most previously tabulated results.

Configuration A was first considered in [2]. It contains a pair of horizontal and a pair of vertical tuning ridges. Fig. 4(a) and (b) shows the dependence of TM- and TE-mode eigenvalues on the penetration of the horizontal pair of tuning ridges. Comparison against tabulated eigenvalues in [2, Fig. 2, Th. I and II] is made in Table II. The agreement is moderate, but the accuracy of the reference is also unspecified. A similar

TABLE III
COMPARISON OF EIGENVALUES FOR CONFIGURATION D AGAINST RESULTS PRESENTED IN [2]

	TE_1		TE_2	
d_c	BIEM	[2]	BIEM	[2]
0.75	1.80096	1.79431	1.88592	1.84835
0.80	1.81160	1.80042	1.86271	1.84519
0.85	1.81980	1.80652	1.84622	1.84169
0.90	1.82517	1.81813	1.83279	1.83787
0.95	1.82762	1.82301	1.82821	1.83633

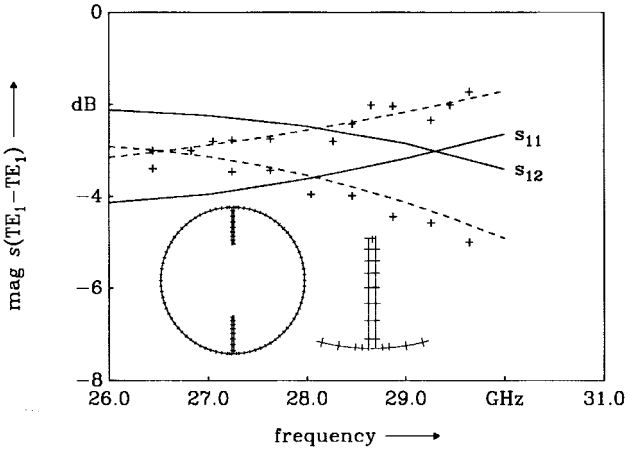

(a)

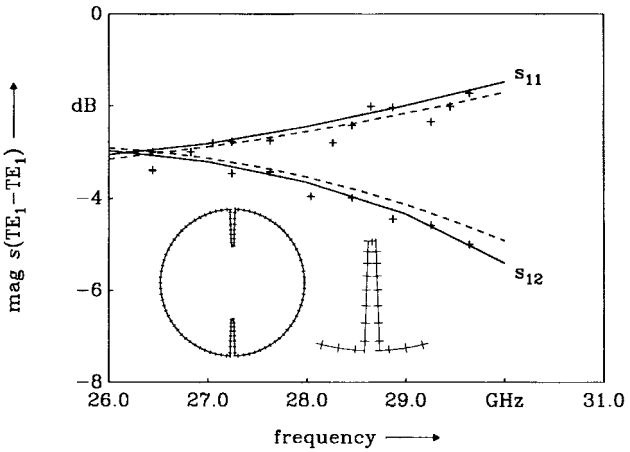

(b)

Fig. 7. Scattering parameters with respect to the CW $TE_{11(0)}$ mode of $0.275 \times r$ long section of (a) MRCW configuration E (rectangular ridges) and (b) MRCW configuration F (conical ridges). Symbols (measurements) and dashed lines (radial mode-matching method) are reproduced from [9, Fig. 3] and identical in both figures.

investigation of parameter dependence of the first few TE-mode eigenvalues of configurations B was first presented in [11]. Fig. 5 gives results for a larger number of modes. Since the reference does not contain numerical values, only qualitative agreement can be confirmed.

Configuration C is another example for which eigenvalues have been previously tabulated in [2, Fig. 2, Th. I and II]. Comparison is made in Table III. As to agreement of results, the same comment applies as to configuration A. The contour discretization for this example is shown in Fig. 3.

TABLE IV
MRCW-MODE EIGENVALUES AND CW-MRCW-MODE COUPLING COEFFICIENTS FOR CONFIGURATION G. FIGURES IN ITALICS ARE ABSOLUTE DIFFERENCES WITH RESPECT TO RESULTS PRESENTED IN [12, Th. II]. THE THIRD CW-MODE INDEX IN COLUMN ONE IS DEFINED BY $\psi_{m,n,i} \sim \cos(m\alpha - i\frac{\pi}{2})$

TM-TM	2.50844	3.90773	4.07273	5.33798	5.78153	6.53081	6.64260	7.15565	7.39397
0,1,0	−0.95003	0.00000	0.00000	0.00000	0.00000	0.00000	0.00000	0.00000	0.00000
	−0.00137								
1,1,0	0.11758	−0.70235	−0.62935	−0.04051	0.06112	0.01257	0.01161	−0.01228	−0.02961
1,1,1	0.12198	0.67418	−0.65543	0.04109	0.06356	−0.01436	0.01039	0.01169	−0.03107
2,1,0	−0.00306	0.12665	−0.00861	−0.93701	−0.01099	0.08621	0.00337	−0.06219	0.00360
2,1,1	0.07033	0.00385	0.19447	−0.01610	0.25071	−0.00270	0.08153	−0.00162	−0.06677
0,2,0	0.09184	0.00058	0.18942	−0.01044	0.85829	−0.00401	0.02233	−0.00084	−0.10826
TM-TE	1.80241	1.87144	2.96832	2.99081	3.79716	3.86141	4.19312	4.90266	5.33038
0,1,0	0.07592	−0.00005	0.06384	0.00768	−0.01644	−0.00023	0.00316	−0.00454	−0.00019
	−0.00279	*0.00000*	*−0.00142*	*−0.00069*					
1,1,0	0.06327	−0.02132	0.06879	−0.03559	−0.03581	0.00006	−0.03267	0.00996	0.00689
1,1,1	0.06600	0.02063	0.06068	0.04879	−0.03063	−0.00070	0.03776	0.00699	−0.00737
2,1,0	−0.00253	−0.04028	0.00781	−0.08081	−0.00488	0.00064	−0.06728	0.00277	0.01288
2,1,1	0.06102	−0.00141	0.10249	0.00673	−0.10785	−0.00077	0.00206	0.05706	−0.00050
0,2,0	0.06517	−0.00005	0.05069	0.00632	−0.00652	−0.00015	0.00256	−0.00864	−0.00010
TE-TE	1.80241	1.87144	2.96832	2.99081	3.79716	3.86141	4.19312	4.90266	5.33038
1,1,0	−0.69744	−0.68470	0.05173	0.03085	−0.02706	0.00918	0.03013	0.01186	−0.00498
	−0.00170	*−0.00074*	*−0.00158*	*−0.00253*					
1,1,1	0.67037	−0.71240	−0.05618	0.01897	0.03184	0.00987	0.02622	−0.01477	−0.00460
	0.00140	*−0.00101*	*0.00237*	*−0.00132*					
2,1,0	−0.00269	−0.00065	−0.91551	−0.07295	−0.27205	−0.00226	0.00260	0.11631	−0.00064
	0.00035	*−0.00002*	*−0.00732*	*0.00773*					
2,1,1	−0.00064	0.01171	0.07570	−0.95185	0.01318	0.02118	0.09589	−0.00499	−0.02036
	0.00003	*0.00080*	*−0.00458*	*−0.00393*					
0,1,0	0.00015	0.02141	−0.00340	0.03062	−0.00668	0.99405	0.02045	−0.00095	0.00362
3,1,0	0.00224	0.00036	−0.06120	0.00625	0.57103	−0.00730	0.65803	0.34640	0.02443

For illustration, the TM and TE boundary-value functions $v'(s)$ and $u''(s)$, which may be identified with the axial and transverse tangential surface current density, respectively, are shown in Fig. 6(a) and (b) for two modes. It is obvious from Fig. 6(a) that the occurrence of the TM-mode field singularities may lend to a substantial increase in the number of CW modes required for the MMNR of the CW–MRCW transition. The singularities may further give rise to increased losses, and thereby deteriorate the accuracy of the perfect electric conductor (PEC) approximation. Singularities can be avoided by use of a smooth ridge shape. Fig. 6(c) illustrates the versatility of the present method in this respect. It shows the function v_1' of MRCW configuration D which contains circular ridges.

MRCW configurations E and F of Table I have previously been considered in [9]. Both contain two very thin vertical ridges with a penetration of half the CW radius and differ only by the shape of the ridges. Configuration E contains rectangular ridges while F contains conical ridges. Measured scattering parameters with respect to the CW $\mathrm{TE}_{11(0)}$ mode of a 0.275 ×radius long section of configuration E are reported in [9, Fig. 3]. However, as a consequence of the restrictions of the radial mode-matching method, configuration F was adopted as an approximation for analysis in [9]. Comparison between both configurations is made in Fig. 7. The agreement between the numerical results [Fig. 7(b)] is very good. For the present calculation, 50 TM and 50 TE modes in MRCW and 200 each in CW were considered. The reference retained 40 modes, each in either waveguide, which explains small differences in Fig. 7(b). Comparison between Fig. 7(a) and (b) reveals the strong sensitivity of results with respect to geometrical parameters. Additional calculations have shown that a variation of ridge length by only0.001 ×radius shifts the 3-dB crossover frequency by more than 4 GHz. The discrepancy between the results is, therefore, probably due to mechanical inaccuracy, as pointed out in [9]. It is obvious that not only is technological reproducibility a challenge, but also that any systematic deviation from the nominal geometry like finite curvature of corners must be accounted for in analyses of this kind.

Configuration G refers to an example recently presented in [12]. This configuration contains one horizontal and one vertical tuning ridge and a single coupling ridge in between. It is the only example for which numerical values of coupling coefficients have been published for a few modes. Comparison against these results is made in Table IV, adopting the sign conventions of the reference. The maximum absolute difference of 0.0077 occurs for the $\mathrm{CW} - \mathrm{TE}_{21(0)}$ to $\mathrm{MRCW} - \mathrm{TE}_4$ coupling coefficient. The rms of the absolute differences for all 21 coefficients is $6.5 \cdot 10^{-4}$.

V. CONCLUSION

A completely contour-based approach to the evaluation of coupling coefficients for abrupt transitions between a standard waveguide and a waveguide of arbitrary cross section has been presented. Numerical results for MRCW and its transition to CW have been compared to most publicly available data for low-order modes. Excellent agreement with the more recently published result by other methods was found.

REFERENCES

[1] M. Guglielmi and G. Gheri, "Rigorous multimode network representation of capacitive steps," *IEEE Trans. Microwave Theory Tech.*, vol. 42, pp. 622–628, Apr. 1994.

[2] M. Guglielmi, R. C. Molina, and A. A. Melcon, "Dual-mode circular waveguide filters without tuning screws," *IEEE Microwave Guided Wave Let.*, vol. 2, pp. 457–458, Nov. 1992.

[3] R. Orta, P. Savi, R. Tascone, and D. Trinchero, "Rectangular waveguide dual-mode filters without discontinuities inside the resonators," *IEEE Microwave Guided Wave Lett.*, vol. 5, pp. 302–304, Sept. 1995.

[4] L. Accantino, G. Bertin, and M. Mongiardo, "A four-pole dual mode elliptic filter realized in circular cavity without tuning screws," *IEEE Trans. Microwave Theory Tech.*, vol. 44, pp. 2680–2687, Dec. 1996.

[5] R. Beyer and F. Arndt, "Field-theory design of circular waveguide dual-mode filters by a combined mode-matching finite element method," in *Proc. 24th European Microwave Conf.*, Cannes, France, Sept. 1994, pp. 294–299.

[6] S. Xiao, R. Vahldieck, and M. Guglielmi, "Field theory analysis of circular ridge waveguides with partial dielectric filling," in *1995 IEEE MTT-S Int. Microwave Symp. Dig.*, vol. 1, Orlando, FL, May 1995, pp. 265–268.

[7] F. Giese, J. M. Reiter, and F. Arndt, "Modal analysis of arbitrarily shaped irises in waveguides by a hybrid contour-integral mode-matching method," in *1995 IEEE MTT-S Int. Microwave Symp. Dig.*, vol. 3, Orlando, FL, May 1995, pp. 1359–1362.

[8] U. Balaji and R. Vahldieck, "Radial mode matching analysis of ridged circular waveguide," in *1995 IEEE MTT-S Int. Microwave Symp. Dig.*, vol. 2, Orlando, FL, May 1995, pp. 637–640.

[9] U. Balaji and R. Vahldieck, "Field theory based s-parameter analysis of circular ridged waveguide discontinuities," in *1996 IEEE MTT-S Int. Microwave Symp. Dig.*, vol. 3, San Francisco, CA, June 1996, pp. 1853–1856.

[10] P. Guillot, P. Couffignal, H. Baudrand, and B. Theron, "Improvement in calculation of some surface integrals: Application to junction characterization in cavity filter design," *IEEE Trans. Microwave Theory Tech.*, vol. 41, pp. 2156–2160, Dec. 1993.

[11] W. Sun and C. A. Balanis, "Analysis and design of quadrupel ridged waveguides," *IEEE Trans. Microwave Theory Tech.*, vol. 42, pp. 2201–2207, Dec. 1994.

[12] P. Arcioni, "Fast evaluation of modal coupling coefficients of waveguide step continuities," *IEEE Microwave Guided Wave Lett.*, vol. 6, pp. 232–234, June 1996.

[13] G. Conciauro, M. Bressan, and C. Zuffada, "Waveguide modes via and integral equation leading to a linear matrix eigenvalue problem," *IEEE Trans. Microwave Theory Tech.*, vol. 32, pp. 1495–1504, Nov. 1984.

[14] W. Schroeder and I. Wolff, "A hybrid-mode boundary integral equation method for normal-and superconducting transmission lines of arbitrary cross section," *Int. J. Microwave Millimeter-Wave CAE*, vol. 2, pp. 314–330, Oct. 1992.

[15] ———, "Full-wave analysis of the influence of conductor shape and structure details on losses in coplanar waveguide," in *1995 IEEE MTT-S Int. Microwave Symp. Dig.*, vol. 3, Orlando, FL, May 1995, pp. 1273–1276.

[16] W. Schroeder and M. Guglielmi, "Boundary integral equation approach to multi-mode y-matrix characterization of multi-ridged sections in circular waveguide," in *1996 IEEE MTT-S Int. Microwave Symp. Dig.*, San Francisco, CA, June 1996, pp. 1849–1852.

[17] W. Schroeder and I. Wolff, "The origin of spurious modes in numerical solutions of electromagnetic field eigenvalue problems," *IEEE Trans. Microwave Theory Tech.*, vol. 42, pp. 644–653, Apr. 1994.

Werner L. Schroeder (M'87) received the Dipl.-Ing. degree in electrical engineering and the Dr.-Ing. degree from Duisburg University, Duisburg Germany, in 1986 and 1993, respectively.

In 1986, he joined the Faculty of Electrical Engineering, Duisburg University, where he has been working on numerical methods for electromagnetic-field analysis with application mainly to active and passive components in MMIC's, on mathematical aspects of numerical methods, and on the physics-based simulation of electronic transport in III–V compound devices. Since 1996, he has been a Member of the Special Research Program "Very High Frequency and Very High Speed Circuits based on III–V-Compound Semiconductors" at Duisburg University. His current research interests focus on the combination of electromagnetic-field analysis and physics-based simulation of electronic transport in heterostructure devices for millimeter-wave applications.

Marco Guglielmi was born in Rome, Italy, on December 17, 1954. He received the Laurea Ingegneria Elettronica degree from the University of Rome La Sapienza, Rome, Italy, in 1979, where in 1980, he attended the Scuola di Specializzazione in Elettromagnetismo Applicato, received the M.S. degree in electrical engineering from the University of Bridgeport, Bridgeport, CT, in 1982, and the Ph.D. degree in electrophysics from Polytechnic University, Brooklyn, NY, in 1986.

From 1984 to 1986, he was an Academic Associate at Polytechnic University, and from 1986 to 1988 was an Assistant Professor. From 1988 to 1989, he was an Assistant Professor at the New Jersey Institute of Technology (NJIT), Newark, NJ. In 1989, he joined the RF System Division, European Space Research and Technology Centre, Noordwijk, The Netherlands, where he is currently involved in the development of passive microwave components for space applications. His professional interests include the areas of solid-state devices and circuits, periodic structures, phased-arrays and millimeter-wave leaky-wave antennas, network representations of waveguide discontinuities, and microwave filtering structures.

Dr. Guglielmi was the recipient of a Fulbright Scholarship and an Halsey International Scholarship Program (HISP) Scholarship in 1981.